

Supplementary Information

Controllable synthesis and structure modulation of ultrafine textured cobalt nanowires

Qing Zhao,^a Jiayue Sun,^a Jiling Zhao,^a Changxin Qi,^{a,b} Ruichao Zhang,^c Zhaonan Yan,^b Wenyang Yu,^a Juan Wen^{*a} and Yong Qin^{*a,b}

^a *Institute of Nanoscience and Nanotechnology, School of Materials and Energy, Lanzhou University, Lanzhou, Gansu 730000, China.*

^b *MIIT Key Laboratory of Complex-field Intelligent Exploration, Beijing Institute of Technology, Beijing 100081, China.*

^c *Lanzhou Jiaotong University, School of Materials Science and Engineering, Lanzhou, Gansu 730000, China*

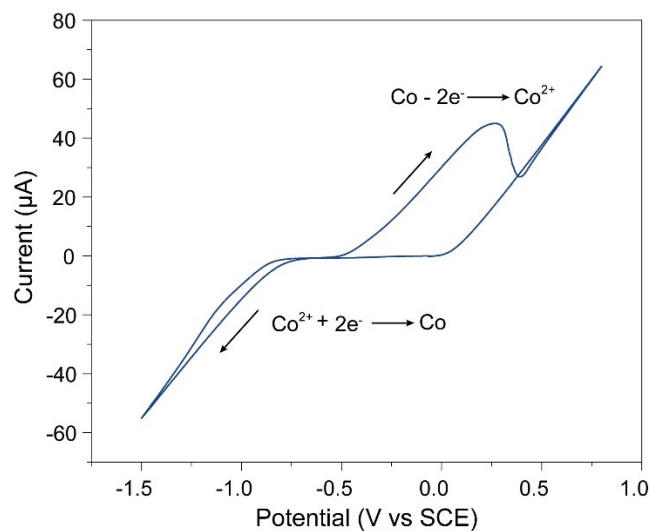


Fig. S1: Cyclic voltammety curve recorded from Co solution used for an electrodeposition of Co nanowires.

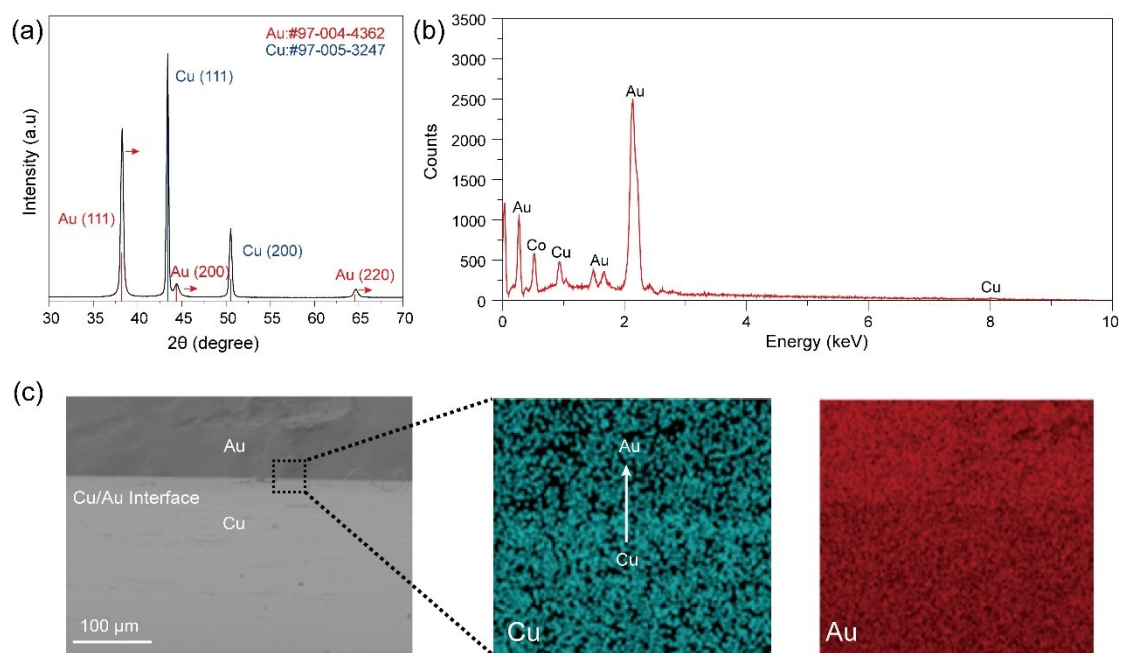


Fig. S2 Structural characterization of the Au–Cu alloy interface. (a) XRD patterns of the Au–Cu alloy interface; (b) EDS spectrum of the Au–Cu alloy interface; (c) Cross-sectional EDS mapping images showing the elemental distribution at the Au–Cu alloy interface.

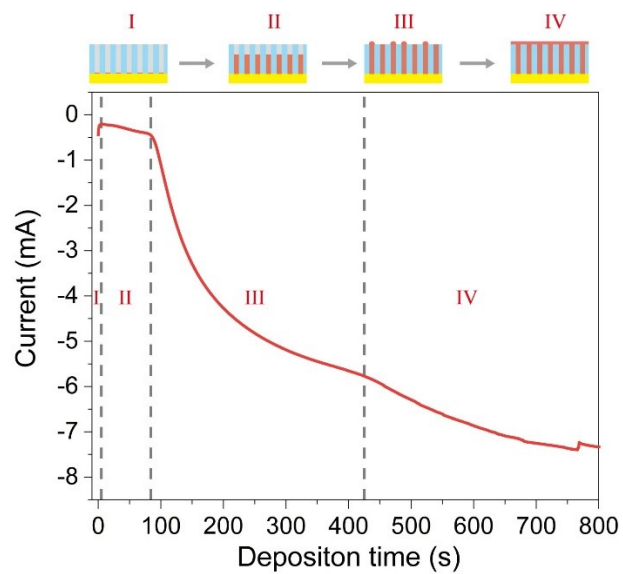


Fig. S3: $I-t$ curve of cobalt nanowires growth process.

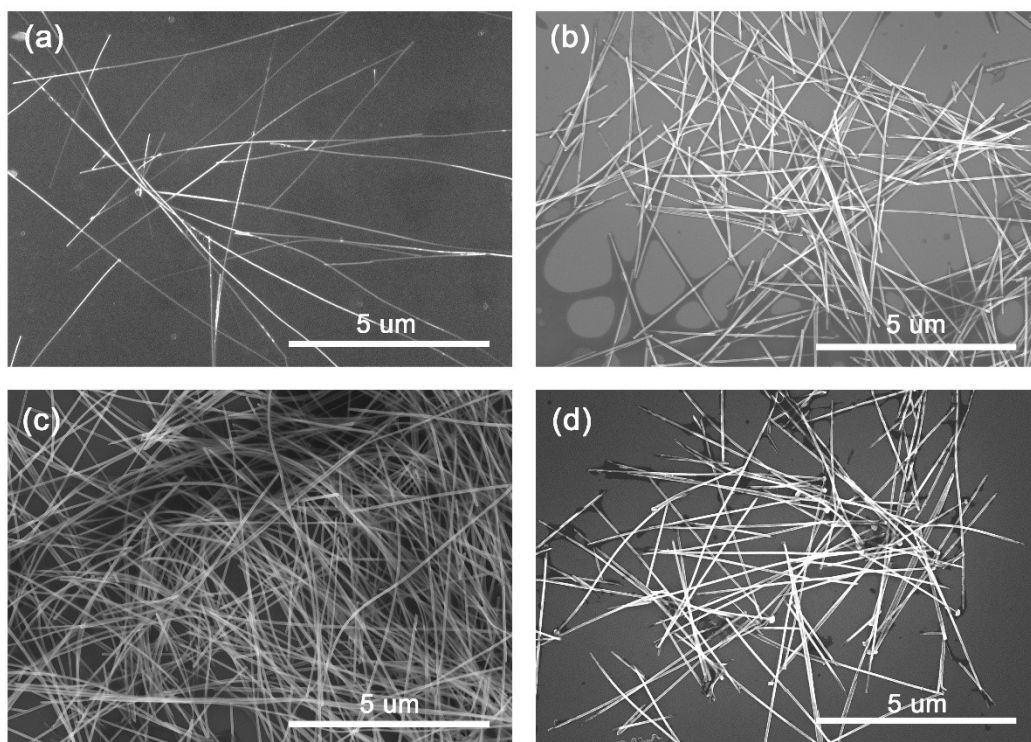


Fig. S4: Morphology of cobalt nanowires with different diameters. (a) 10 nm; (b) 30 nm; (c) 50 nm; (d) 80 nm.

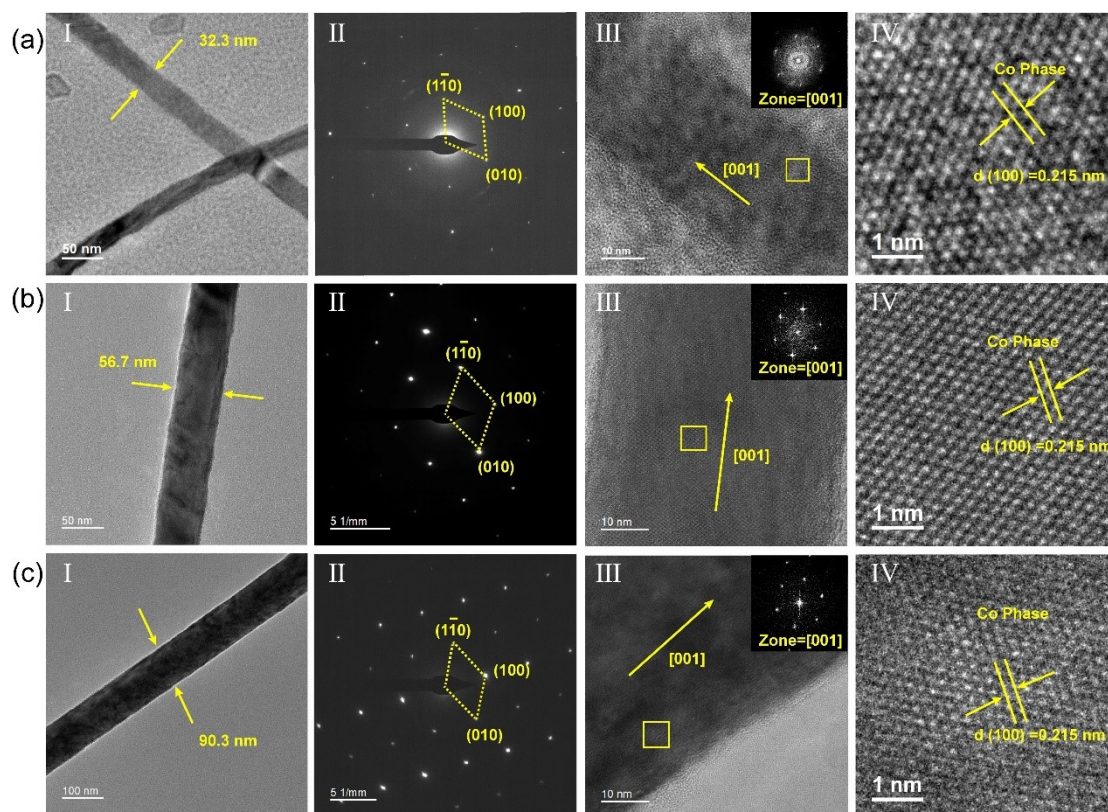


Fig. S5 Diameter-independent single-crystal-like electrodeposited Co nanowires. (a-c(I)) TEM images of Co nanowires with various diameters (30 nm, 50 nm, and 80 nm); (a-c(II)) the corresponding SAED patterns of Co nanowires with various diameters (30 nm, 50 nm, and 80 nm); (a-c(III-IV)) HRTEM images of Co nanowires with various diameters (30 nm, 50 nm, and 80 nm).

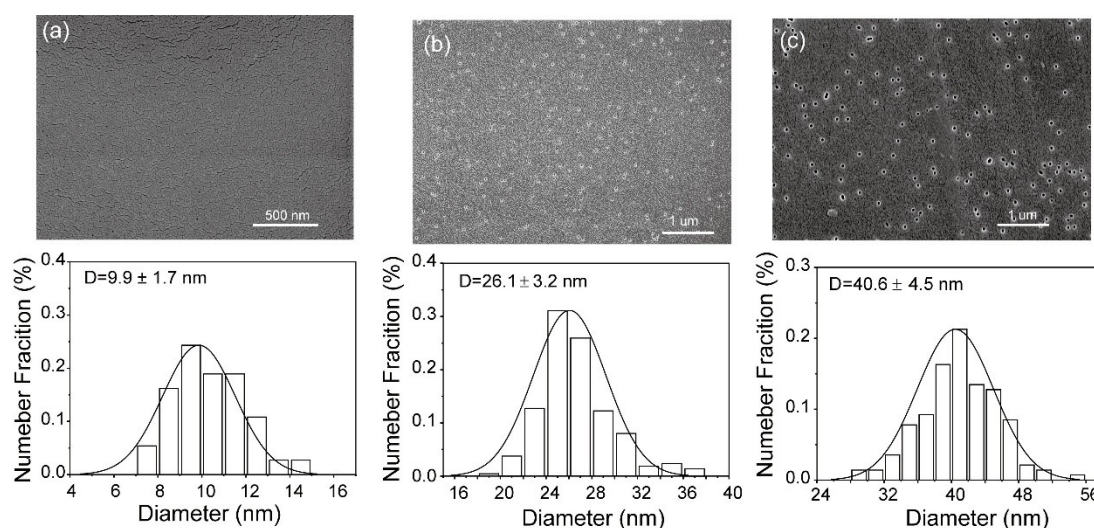


Fig. S6: Different template morphology and pore size distribution. (a) 10 nm; (b) 30 nm; (c) 50 nm.

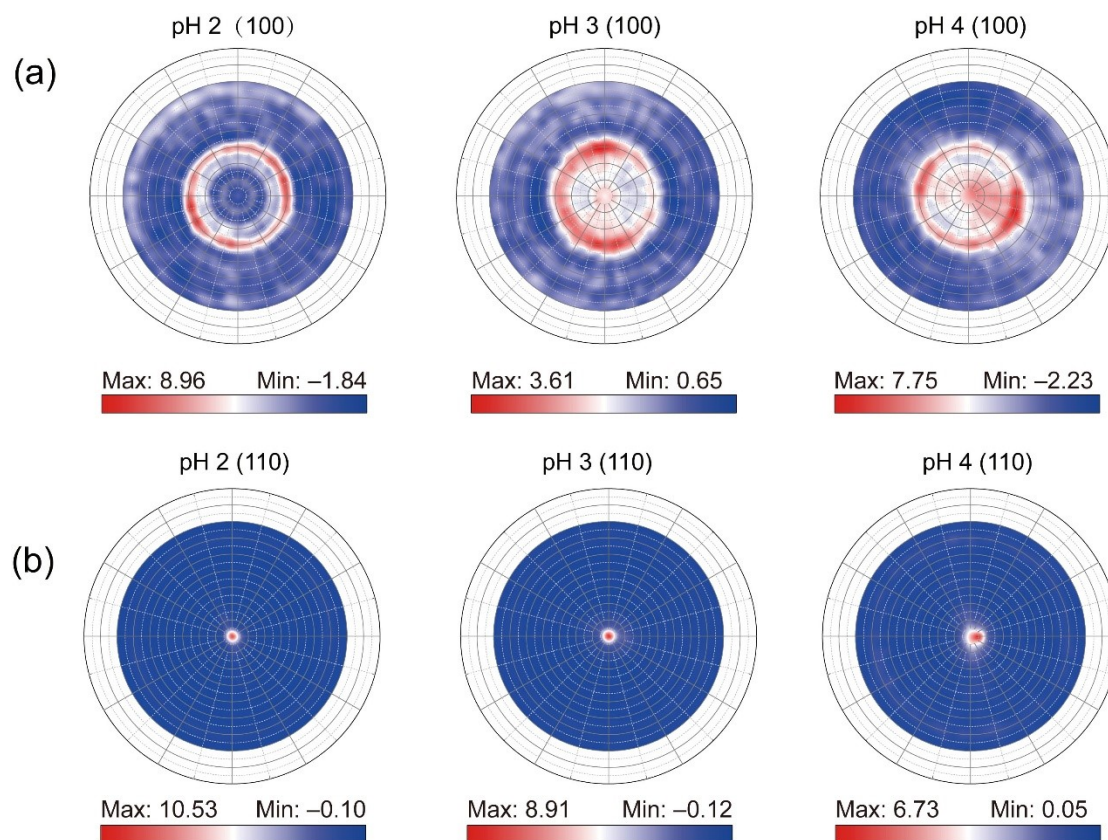


Fig.S7 XRD pole figures of cobalt nanowires synthesized under varying pH conditions. (a) Pole figures of the (100) crystal plane and (b) pole figures of the (110) crystal plane.

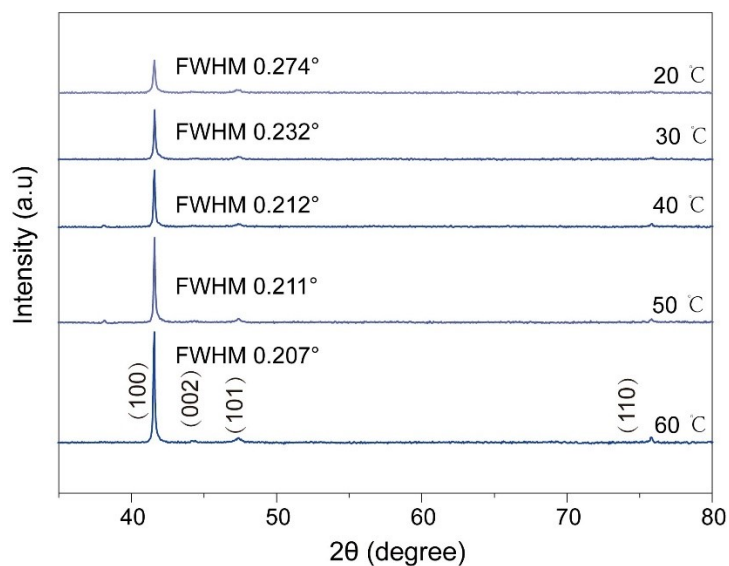


Fig. S8: XRD of cobalt nanowires at different temperatures.

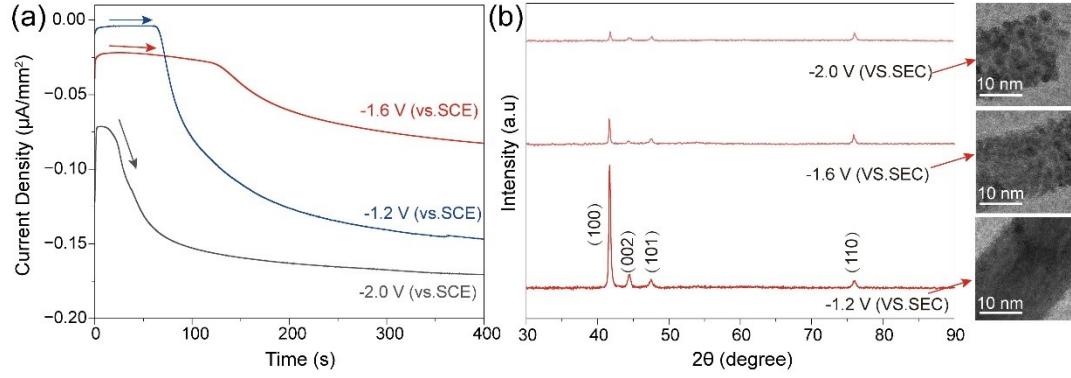


Fig. S9 Influence of deposition potential on the growth dynamics and crystalline quality of Co nanowire arrays; (a) Chronoamperometric curves for Co nanowire deposition at potentials ranging from -1.2 V to -2.0 V (vs. SCE); (b) The corresponding XRD patterns and TEM images.

Method S1: Finite element simulation (COMSOL Multiphysics)

The use of finite element simulation software (COMSOL Multiphysics) to model electrochemical deposition Co process deepens the understanding the localized electrochemical.

The flux for each of the ions in the electrolyte is given by the Nernst–Planck equation:

$$N_i = -D_i \nabla c_i - z_i u_i F c_i \nabla \phi_l$$

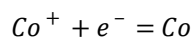
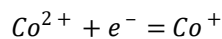
where N_i denotes the transport vector ($\text{mol}/(\text{m}^2 \cdot \text{s})$), c_i the concentration in the electrolyte (mol/m^3), z_i the charge for the ionic species, u_i the mobility of the charged species ($\text{m}^2/(\text{s} \cdot \text{J} \cdot \text{mole})$), F Faraday's constant (As/mole), and ϕ_l the potential in the electrolyte (V). The material balances are expressed through:

$$\frac{\partial c_i}{\partial t} + \nabla \cdot N_i = 0$$

one for each species, that is $i = 1, 2$. The electroneutrality condition is given by the following expression:

$$\sum_i z_i c_i = 0$$

The boundary conditions for the anode and cathode are given by the Butler–Volmer equation for copper deposition. The deposition process is assumed to take place through the following simplified mechanism:



where the first step is rate determining step, RDS, and the second step is assumed to be at equilibrium ¹. This gives the following relation for the local current density as a function of potential and copper concentration:

$$i_{ct} = i_0 \left(\exp\left(\frac{1.5F\eta}{RT}\right) - \frac{u_{Co^{2+}}}{u_{Co^{2+},ref}} \exp\left(\frac{1.5F\eta}{RT}\right) \right)$$

where: i_0 is the exchange current density, η denotes the overpotential defined as:

$$\eta = \phi_{s,0} - \phi_l - \Delta\phi_{eq}$$

where $\phi_{s,0}$ denotes the electronic potential of the respective electrode. This gives the following condition for the cathode:

$$N_{Co^{2+}} \cdot n = -\frac{i_0}{2F} \left(\exp\left(\frac{1.5F(\phi_{s,cat} - \phi_l - \Delta\phi_{eq})}{RT}\right) - \frac{c_{Co^{2+}}}{c_{Co^{2+},ref}} \exp\left(\frac{0.5F(\phi_{s,cat} - \phi_l - \Delta\phi_{eq})}{RT}\right) \right)$$

where n denotes the normal vector to the boundary. The condition at the anode is

$$N_{Co^{2+}} \cdot n = -\frac{i_0}{2F} \left(\exp\left(\frac{1.5F(\phi_{s,cat} - \phi_l - \Delta\phi_{eq})}{RT}\right) - \frac{c_{Co^{2+}}}{c_{Co^{2+},ref}} \exp\left(\frac{0.5F(\phi_{s,an} - \phi_l - \Delta\phi_{eq})}{RT}\right) \right)$$

All other boundaries are insulating:

$$N_{Co^{2+}} \cdot n = 0$$

For the sulfate ions, insulating conditions apply everywhere:

$$N_{SO_4^{2-}} \cdot n = 0$$

The initial conditions set the composition of the electrolyte according to

$$c_{Co^{2+}} = c_0$$

$$c_{SO_4^{2-}} = c_0$$

In the finite element analysis (FEA), the simulation model was simplified to comprise the electrolyte solution, cathode, anode, and insulator. The electrolyte used was 500 mol/m³ cobalt sulfate (CoSO₄). In the simulation, the red region represents the cathode substrate, to which a potential of -0.135 V was applied. The black region represents the anode, to which a potential of 0.135 V was applied.

Method S2: DFT calculation method

The adsorption energy of H⁺ on the Co surface was calculated using Density Functional Theory (DFT) as implemented in the CASTEP module. The calculations employed the generalized gradient approximation (GGA) with the Perdew-Burke-Ernzerhof (PBE) functional for exchange-correlation interactions, along with norm-conserving

pseudopotentials. A plane-wave basis set with a kinetic energy cutoff of 500 eV was used, and the Brillouin zone was sampled using a $3 \times 2 \times 1$ k-point grid. The convergence criteria were set as follows: total energy change of 2.0×10^{-5} eV/atom, maximum residual force of 0.05 eV/Å, maximum stress of 0.1 GPa, and maximum displacement of 0.002 Å. Additionally, the self-consistent field (SCF) convergence threshold was set to 2.0×10^{-6} eV/atom.

Surface energy calculation:

$$\sigma = \frac{E_{slab}^N - N * E_{bulk}}{2S}$$

Here, E_{slab}^N , N , E_{bulk} , S are the total energy of slab, the number of atoms constituting the slab model, the energy of a single atom, and the surface area of the exposed crystal plane.

The adsorption energy E_{ads} of H^+ is calculated as follows :

$$E_{ads} = E_{total} - E_{slab} - E_{H^+}$$

Here, E_{slab}^N , N , E_{bulk} , S are the total energy of slab adsorbing, the energy of slab model, and the energy of H^+ is -0.27 ev.

Table S1: Calculation results of (100) crystal plane and (110) crystal plane

crystal plane	surface energy (eV)	Surface area (Å ²)	Average surface formation energy (J/ Å ²)	Proton correction
(100)	2.60	71.49	0.58	-7.24
(110)	1.49	61.91	0.39	-6.86

Reference

1. Mattsson, E., & Bockris, J. M., *Trans. Faraday Soc.*, 1959,**55**, 1586-1601.